



HAL
open science

Ultrahigh-Field Multimodal MRI Assessment of Muscle Damage

Alexandre Fouré, Lauriane Pini, Stanislas Rappacchi, Augustin C. Ogier, Jean-Camille Mattei, Mark Bydder, Maxime Guye, David Bendahan

► **To cite this version:**

Alexandre Fouré, Lauriane Pini, Stanislas Rappacchi, Augustin C. Ogier, Jean-Camille Mattei, et al.. Ultrahigh-Field Multimodal MRI Assessment of Muscle Damage. *Journal of Magnetic Resonance Imaging*, 2019, 49 (3), pp.904-906. 10.1002/jmri.26222 . hal-02459104

HAL Id: hal-02459104

<https://univ-lyon1.hal.science/hal-02459104>

Submitted on 6 Sep 2024

HAL is a multi-disciplinary open access archive for the deposit and dissemination of scientific research documents, whether they are published or not. The documents may come from teaching and research institutions in France or abroad, or from public or private research centers.

L'archive ouverte pluridisciplinaire **HAL**, est destinée au dépôt et à la diffusion de documents scientifiques de niveau recherche, publiés ou non, émanant des établissements d'enseignement et de recherche français ou étrangers, des laboratoires publics ou privés.

Ultrahigh-Field Multimodal MRI Assessment of Muscle Damage

Alexandre Fouré,^{1,2,3} Lauriane Pini,^{1,2}
Stanislas Rappacchi,¹ Augustin C. Ogier,⁴
Jean-Camille Mattei,^{1,2,5} Mark Bydder,^{1,2,6}
Maxime Guye,^{1,2} and David Bendahan¹

To The Editor:

Magnetic resonance imaging (MRI) is a powerful tool to assess skeletal muscle damage both in injured athletes and patients with neuromuscular diseases. Alterations in muscle have been assessed with T_2 -weighted,¹ diffusion tensor,² and sodium MRI.³ However, these sequences require a high signal-to-noise ratio. Considering these limitations, one could expect that measurements performed at ultrahigh-field strength (eg, 7T) would provide a more accurate assessment of skeletal muscle diffusivity properties⁴ and sodium concentration⁵ so that relevant information regarding changes in biochemical and structural tissues properties related to muscle damage may be obtained.

A 33-year-old man (188 cm, 82 kg) volunteered to participate in the study after providing informed consent. Calf muscles were injured during a high-intensity electrostimulation exercise performed using a commercial device (Compex Performance, Djo global, France). Muscle MRI was performed using a whole-body scanner (Magnetom 7T, Siemens Healthcare, Erlangen, Germany). Five days after the damaging exercise, a multimodal imaging session was performed. High-resolution T_1 -weighted images (a gradient-recalled echo [GRE] with parameters previously detailed⁴ and a turbo spin-echo, repetition time [TR] = 3500 msec, echo time [TE] = 34 msec, in-plane field of view [FoV] = 180×180 mm², matrix = 640×640 , 15 slices, ST = 6 mm, gap between slice = 6 mm, bandwidth = 230 Hz/px, TA = 240 sec) were acquired and the corresponding images were used as anatomical reference images. A multiecho GRE sequence (TR = 43 msec, TEs = 3.57/8.51/13.60/18.69/23.78/28.87/33.96/39.05 msec, flip angle = 10°, in-plane FoV = 180×180 mm², matrix = 448×448 , 60 slices, ST = 3 mm, bandwidth = 370 Hz/px, TA = 456 sec) was used to produce T_2^* maps, while T_2 maps were generated from T_2 -weighted images acquired with a segmented (15 segments) echo planar imaging sequence with TEs = 8/18/28/38/48/58 msec. Other acquisition parameters were as follows: FoV = 180×180 mm²; matrix = 192×192 ; TR = 4800 msec; 20 slices; ST = 6 mm; gap between slices = 6 mm, short-tau inversion-recovery for fat saturation; TA for each TE = 132 sec. Axial multidirectional diffusion-weighted images with fat saturation were acquired to characterize diffusion tensor imaging derived parameters as previously described.⁴ A 3D radial sequence was used to obtain sodium images using the following parameters: TR = 110 msec, TE = 0.2 msec, FoV = $180 \times 180 \times 180$ mm³, voxel resolution = $2 \times 2 \times 2$ mm³, 10^4 radial

spokes, bandwidth = 276 Hz/px, TA = 1102 sec. High-resolution T_1 -weighted images were used as reference images (GRE, TR = 13 msec, TE = 5 msec, in-plane FoV = 180×180 mm², matrix = 512×512 , 88 slices, ST = 2 mm, bandwidth = 260 Hz/px, TA = 587 sec). Sodium images were acquired in the presence of six calibration phantoms with different sodium concentrations (10, 30, and 50 mM) and placed within the FoV. Images were then corrected from B_1 inhomogeneities using precalibrated B_1 sensitivity maps from a phantom acquisition measured using the phase sensitive method.⁶

Additional investigations were performed at 1.5T (Avanto, Siemens Healthcare) in order to quantify muscle T_2 values averaged on all slices 3 (D3), 5 (D5), 7 (D7), and 14 (D14) days after the damaging exercise, as previously described.⁷ Control muscle T_2 values were determined 6 months (M6) after the damaging exercise.

As illustrated in Fig. 1a, 1.5T measurements showed an increased T_2 value in gastrocnemius medialis reaching the highest intensity 5 days after the damaging exercise and being resolved after a 6-month period. A slight T_2 increase was observed in the soleus at D3 but no other changes could be seen in antagonist muscles. Ultrahigh-field MRI measurements confirmed the T_2 increase (Fig. 1b) and extended our knowledge, showing concomitant local changes in T_2^* and sodium concentration (in comparison to unaffected muscles, eg, lateral compartment of the lower leg) in addition to transverse diffusivity (λ_3) and fractional anisotropy (FA) as compared to published control values.⁴ In addition, diffusion parameters were increased in other areas, ie, FA and sodium concentration in the gastrocnemius lateralis, eigenvalues (λ_1 , λ_2 , λ_3), mean diffusivity (MD), T_2^* , and sodium concentration in the anterior compartment of the lower leg muscles (Fig. 1c).

The 7T MRI measurements showed additional changes in the same muscle regarding diffusion properties and sodium concentration together with changes in agonist and antagonist muscles that were not visible from the 1.5T measurements.

Studies have previously reported T_2 changes resulting from damaging exercise and assigned them to inflammatory/edematous processes.¹ Changes in DTI metrics have been reported in the early phase of muscle damage,⁸ illustrating subtle alterations of muscle diffusion properties. Sodium MRI can provide further information regarding biochemical changes in the damaged muscle, as recently shown in Achilles tendon⁹ and knee cartilage.¹⁰

From 1.5T MRI measurements, a large T_2 increase was quantified in the gastrocnemius medialis muscle as a result of the damaging muscle stimulation. Interestingly, measurements performed at higher field (7T) confirmed the T_2 changes but also illustrated changes in agonist and antagonist muscles that were not detected at 1.5T. Larger diffusion parameters values were measured in the anterior compartment of the lower leg muscles, thereby suggesting subtle changes in the diffusion properties. These changes could be

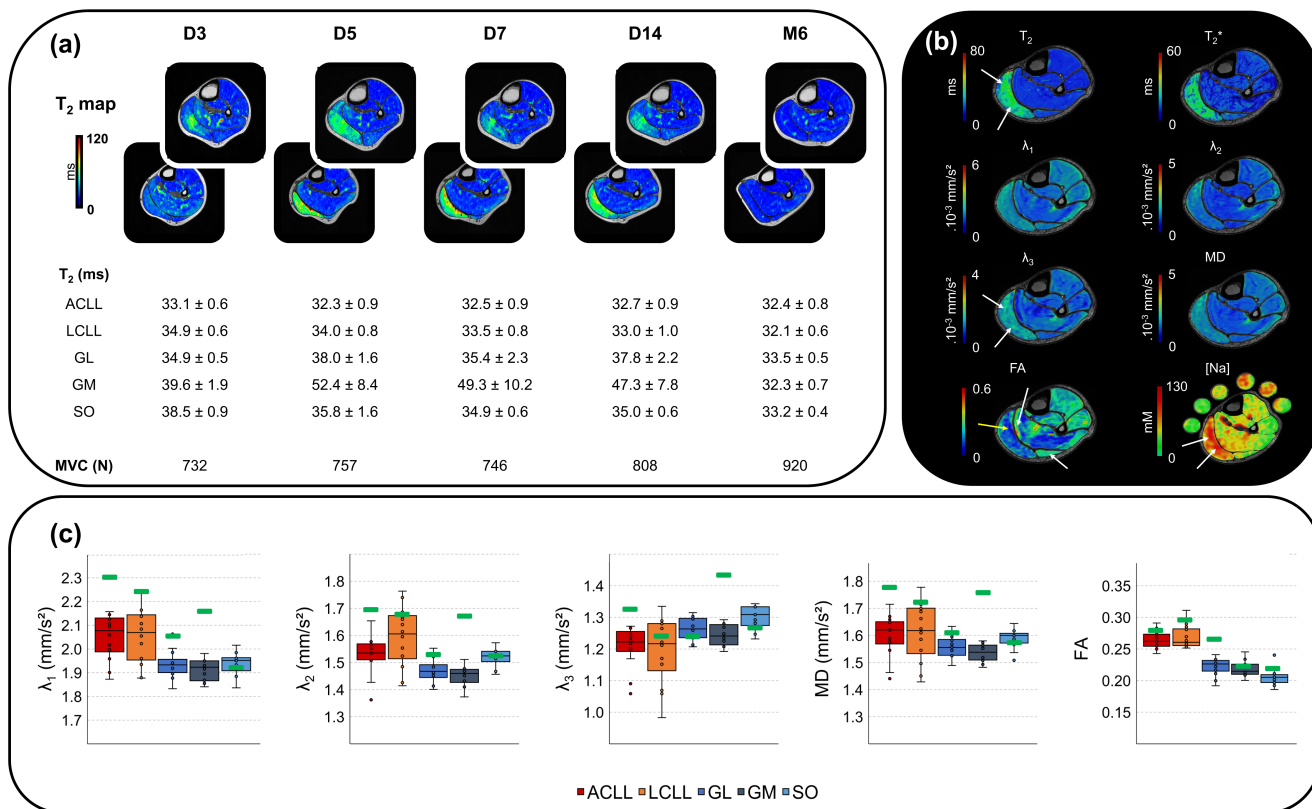


FIGURE 1: (a) T_2 maps overlaid on anatomic images recorded at 1.5T for a proximal and a distal slice of the lower leg. Mean T_2 values for the triceps surae muscles (gastrocnemius medialis [GM], gastrocnemius lateralis [GL], and soleus [SO]) and the muscles from the lateral and the anterior compartments of the lower leg (LCLL and ACLL, respectively), and maximal voluntary isometric plantarflexion force (MVC) determined 3 days (D3), 5 days (D5), 7 days (D7), 14 days (D14), and 6 months (M6) after the neuromuscular electrical stimulation exercise inducing muscle damage are specified below. (b) Quantitative maps of T_2 , T_2^* , diffusion tensor-derived parameters (λ_1 , λ_2 , λ_3 , mean diffusivity [MD], fractional anisotropy [FA]) and sodium concentration ([Na]) overlaid on transverse anatomical images of the lower leg muscles recorded 5 days after the damaging exercise at 7T. Arrows indicate local changes in T_2 , T_2^* , λ_3 , FA, and [Na] (yellow arrow: decrease, white arrow: increase). Specific localized changes in FA and [Na] are displayed, suggesting a specific characterization of muscle structure and biochemical environment, respectively. The sodium concentration and T_2^* averaged on all slices were 63 ± 16 mM and 22.5 ± 5.2 msec for the GM, 27 ± 7 mM and 13.9 ± 4.9 msec for the GL, 32 ± 7 mM and 15.2 ± 1.9 msec for the soleus, 15 ± 6 mM and 15.1 ± 2.3 msec for the LCLL, and 27 ± 11 mM and 16.3 ± 1.8 msec for the ACLL. (c) Diffusion tensor imaging-derived parameters (green marker) including eigenvalues (λ_1 , λ_2 , λ_3), mean diffusivity (MD) and fractional anisotropy (FA) of the triceps surae muscles (gastrocnemius medialis [GM], gastrocnemius lateralis [GL] and soleus [SO]) and the muscles from the lateral and the anterior compartments of the lower leg (LCLL and ACLL, respectively) for the case subject superimposed on boxplots of values obtained in 14 healthy controls from a previous study.⁴

explained by muscle co-contraction of agonist and antagonist muscles during the damaging exercise and/or muscle balance modification leading to overcompensation of the undamaged muscles. In addition, an increased FA was observed in the neighboring soleus muscle area, which could be due to the stress mediated by the increased muscle volume of the gastrocnemius medialis associated with the edema/inflammation processes.

In conclusion, multimodal 7T MR of skeletal muscle shows potential. Performed in a larger number of subjects, the corresponding longitudinal changes could provide a better understanding of the physiopathological mechanisms underpinning muscle tissue alteration and regeneration and of the intramuscular changes that are driving T_2 changes. This ultrahigh-field MRI multimodal approach could be helpful in athletes and patients with neuromuscular disorders for the assessment of biochemical and/or microstructural changes occurring in skeletal muscle after injuries, during sport reconditioning, and in case of surgical intervention.

Acknowledgments

This study was supported by Centre National de la Recherche Scientifique (CNRS UMR 7339). The authors thank Dr. Pierre Besson and Dr. Guillaume Duhamel for help in data analysis, Dr. Thorsten Feiweier for DTI explorations and the Assistance Publique des Hôpitaux de Marseille (APHM). Grant support: Supported by the French IA Equipex 7T-AMI ANR-11-EQPX-0001, A*MIDEX-EI-13-07-130115-08.38-7TAMISTART, A*MIDEX ANR-11-IDEX-0001-02.

¹Aix-Marseille University CNRS, CRMBM, Marseille, France
²APHM Hôpital Universitaire Timone, CEMEREM, Marseille, France
³Laboratoire Interuniversitaire de Biologie de la Motricité, Université Claude Bernard Lyon 1, Villeurbanne, France
⁴Aix-Marseille University Université de Toulon, CNRS, LIS, Marseille, France
⁵APHM Hôpital Nord, Service d'Orthopédie, Marseille, France
⁶University of California David Geffen School of Medicine, Department of Radiological Sciences Los Angeles, California, USA

References

1. Arpan I, Forbes SC, Lott DJ, et al. T(2) mapping provides multiple approaches for the characterization of muscle involvement in neuromuscular diseases: a cross-sectional study of lower leg muscles in 5-15-year-old boys with Duchenne muscular dystrophy. *NMR Biomed* 2013;26:320–328.
2. Hooijmans MT, Damon BM, Froeling M, et al. Evaluation of skeletal muscle DTI in patients with Duchenne muscular dystrophy. *NMR Biomed* 2015;28:1589–1597.
3. Weber MA, Nagel AM, Wolf MB, et al. Permanent muscular sodium overload and persistent muscle edema in Duchenne muscular dystrophy: a possible contributor of progressive muscle degeneration. *J Neurol* 2012; 259:2385–2392.
4. Fouré A, Ogier AC, Le Troter A, et al. Diffusion properties and 3D architecture of human lower leg muscles assessed with ultra-high-field-strength diffusion-tensor MR imaging and tractography: reproducibility and sensitivity to sex difference and intramuscular variability. *Radiology* 2018;287: 592–607.
5. Trattnig S, Zbyn S, Schmitt B, et al. Advanced MR methods at ultra-high field (7 Tesla) for clinical musculoskeletal applications. *Eur Radiol* 2012; 22:2338–2346.
6. Morrell GR. A phase-sensitive method of flip angle mapping. *Magn Reson Med* 2008;60:889–894.
7. Fouré A, Le Troter A, Guye M, Mattei JP, Bendahan D, Gondin J. Localization and quantification of intramuscular damage using statistical parametric mapping and skeletal muscle parcellation. *Sci Rep* 2015;5:18580.
8. Heemskerk AM, Strijkers GJ, Drost MR, van Bochove GS, Nicolay K. Skeletal muscle degeneration and regeneration after femoral artery ligation in mice: monitoring with diffusion MR imaging. *Radiology* 2007;243: 413–421.
9. Juras V, Winhofer Y, Szomolanyi P, et al. Multiparametric MR imaging depicts glycosaminoglycan change in the Achilles tendon during ciprofloxacin administration in healthy men: initial observation. *Radiology* 2015;275:763–771.
10. Trattnig S, Bogner W, Gruber S, et al. Clinical applications at ultrahigh field (7 T). Where does it make the difference? *NMR Biomed* 2016;29: 1316–1334.

DOI: 10.1002/jmri.26222

Level of Evidence: 5

Technical Efficacy Stage: 3